

PROPERTIES OF EAS GONIOMETER AIP

All definitions of the values and functions used see in the part «**GONIOMETER'S GENERIC PROPERTIES**»

The AIP goniometer is operating now

E. Andronikashvili Institute of Physics under Tbilisi State University, Tbilisi, Georgia



Location of the AIP installation

Latitude	41.720500°N
Longitude	44.743882°E
Altitude	(495 ± 5)m above sea level
Upright atmospheric mass depth	$X_{\text{AIP}}^{\uparrow} = 972.8 \text{ g/cm}^2$
Air density at this location	$\rho_{\text{AIP}} = 1167 \text{ g/m}^3$
and the corresponding multiple scattering unit	$rM_{\text{AIP}} = 82.4m$

The “pyramidal” detectors of AIP goniometer are located under the concrete roof of second building of Andronikashvili Institute of Physics in Tbilisi. The mass depth of this filter is accepted to be $X_{\text{filter}} = 30.8 \text{ g/cm}^2$ for all directions and the radiation length for the actual absorber’s substance is accepted to be $T_{\text{filter}} = 27.5 \text{ g/cm}^2$

Number of detectors $N = 4$; $d = 0, 1, 2, 3$

The areas of all plastic scintillator slabs are $S_d = 0.25\text{m}^2$; $\{SS_{\text{AIP}}\} = (S_0, S_1, S_2, S_3,)$

The detectors' positions layout in the roof space is shown in the **figure 1**.

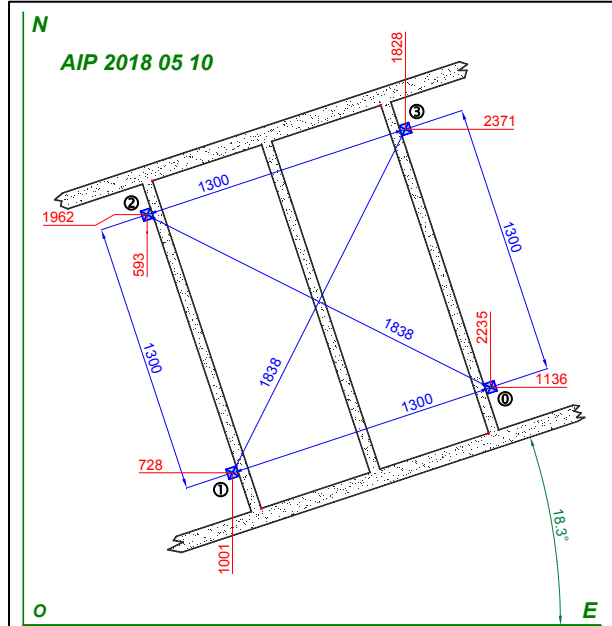


Figure 1. AIP array layout.
All linear dimensions are measured in centimeters.

Local $(E, N)^T$ coordinates of the detectors are obtained by two-dimensional multilateration procedure relative to the fixed points on the circumscribing walling with subsequent rotation by 18.3° about the vertical axis:

$$\{\mathbf{rr}_{\text{AIP}}\} = \begin{pmatrix} 2235 & 1001 & 593 & 1828 \\ 1136 & 728 & 1962 & 2371 \end{pmatrix} \text{cm} \quad \begin{array}{l} "E" \\ "N" \end{array}$$

The practically occurred EAS observation rate at AIP goniometer's performance during the 2020 year observation session is

$$\text{ExpRate}_{\text{AIP}} = (2.663 \pm 0.088) \text{ hr}^{-1}.$$

The required effective common threshold of sensitivity n_{AIP}^* of all detectors used is estimated by numerical solving of the equation

$$\widehat{\text{Rate}}(n_{\text{AIP}}^*) = \text{ExpRate}_{\text{AIP}}$$

shown in the **figure 2**. Here $\widehat{\text{Rate}}(n^*)$ is the interpolation polynomial curved upon the set of calculated rates for the series of arbitrarily assigned values n^* of supposed thresholds of sensitivity. The effective common threshold of sensitivity of all detectors is estimated as $n_{\text{AIP}}^* = 8.1563$ particles per detector.

Therefore the aggregate variable AIP describing the native properties of the AIP goniometer is established as $AIP = [X_{\text{AIP}}^\uparrow, \{\mathbf{rr}_{\text{AIP}}\}, \{SS_{\text{AIP}}\}, \{nn_{\text{AIP}}^*\}]$. Every consequent calculation uses this set of properties.

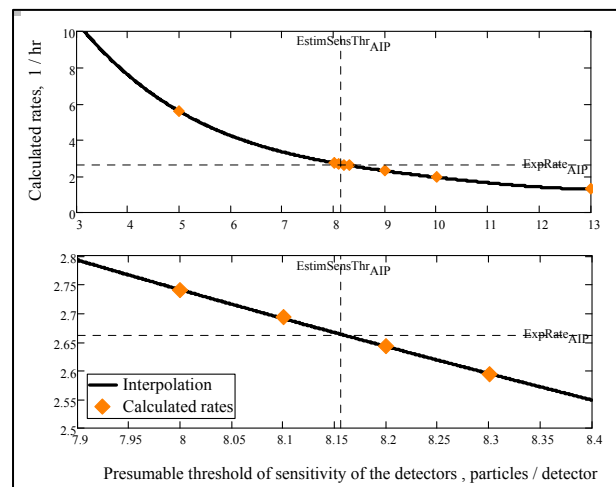


Figure 2 Plot of the numerical estimation of the effective common threshold of sensitivity of the detectors of AIP goniometer.

The properties evaluated

The calculated rate of EAS observations by AIP goniometer is $\text{Rate}_{\text{AIP}} = 2.663 \text{ hr}^{-1}$ while the observations rate is $\text{ExpRate}_{\text{AIP}} = (2.663 \pm 0.088) \text{ hr}^{-1}$.

The aperture function of the AIP goniometer

The estimated dependence of the AIP goniometer's aperture ${}^{(AIP)}\text{Ap}(E)$ on the showers' energy E is shown in the **figure 3**.

The lower energy threshold of the observable EAS events is

$$\begin{aligned} {}^{(AIP)}E_{\text{thr}} &= 7.7 \times 10^5 \text{ GeV} \\ &= 7.7 \times 10^{14} \text{ eV} \end{aligned}$$

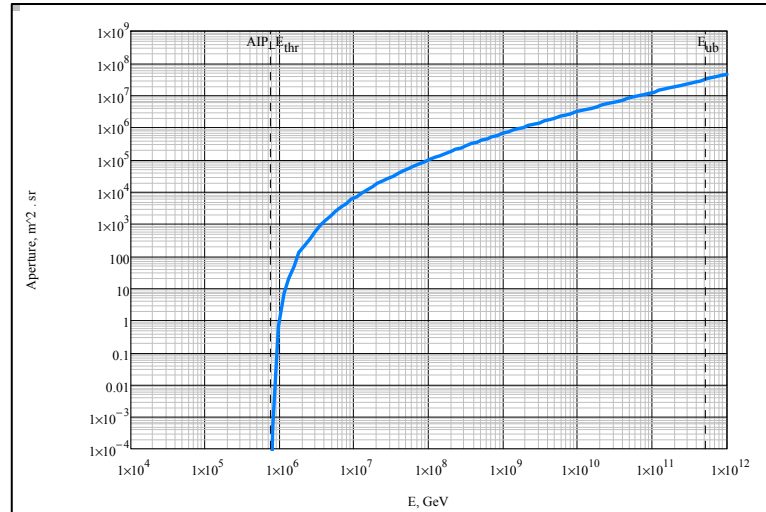


Figure 3. Dependence of the AIP goniometer's aperture on the showers' energy E

The probability density function of the EAS energies observable by the AIP goniometer

The estimated density function of the EAS energies E observable by the AIP goniometer ${}^{(AIP)}f_E(E)$ is shown in the **figure 4**.

The average energy of the observable showers is

$$\begin{aligned} {}^{(AIP)}E_{av} &= 2.5 \times 10^7 \text{ GeV} \\ &= 2.5 \times 10^{16} \text{ eV} \end{aligned}$$

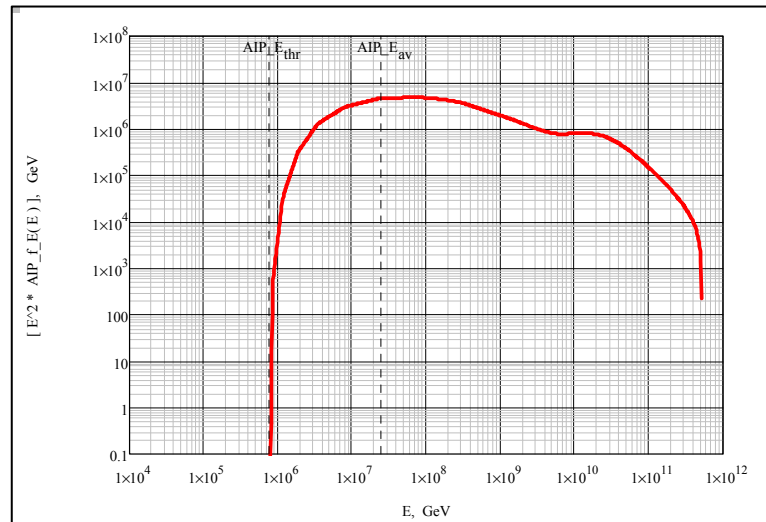


Figure 4. The EAS energy E distribution density for AIP goniometer observations is shown. Density values are scaled by corresponding energy E in the power 2.0

The integral distribution function of the EAS energies observable by the AIP goniometer

The estimated total number of EAS events observable by AIP goniometer in the course of 1 year ${}^{(AIP)}F_E(E_{min})$ dependent on the minimal energy E_{min} of the showers' sampling part is shown in the **figure 5**.

Total rate of all showers observation is

$$\begin{aligned} {}^{(AIP)}Rate_{tot} &= 23347 \text{ EAS/year} \\ &= 2.663 \text{ EAS/hr} \end{aligned}$$

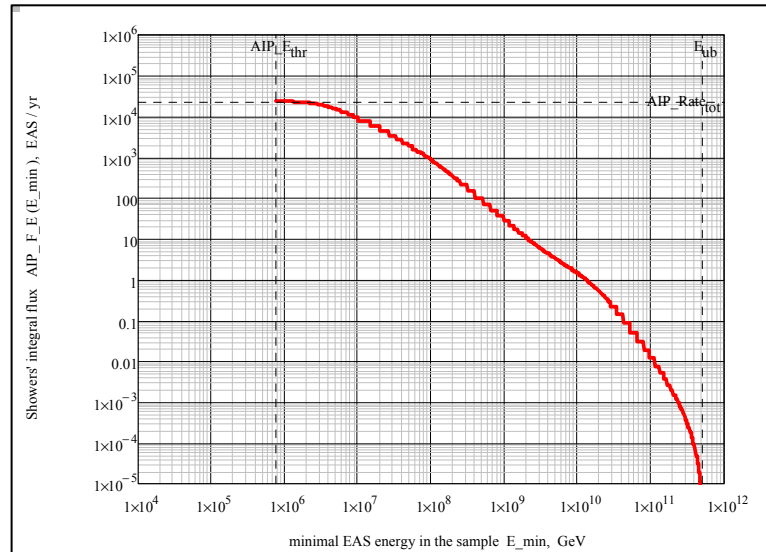


Figure 5. The curve shows the dependence on the sample minimal energy of total number of EAS events observable by AIP goniometer in the course of 1 year

The greatest accessible distance to the shower cores

The function ${}^{(AIP)}R_{\max}(E)$ of the greatest accessible distance to the shower cores is defined numerically at given energy. This function is shown in the **figure 6**.

This dependence is defined in the energy interval

$${}^{(AIP)}E_{\text{thr}} < E < {}^{(AIP)}E_{\text{ub}}$$

The maximal available distance is defined at upper bound of observable EAS energy

$$E_{\text{ub}} = 516 \text{ EeV} = 5.16 \times 10^{20} \text{ eV}$$

$${}^{(AIP)}\text{maxR} = {}^{(AIP)}R_{\max}(E_{\text{ub}}) = 2194 \text{ m}$$

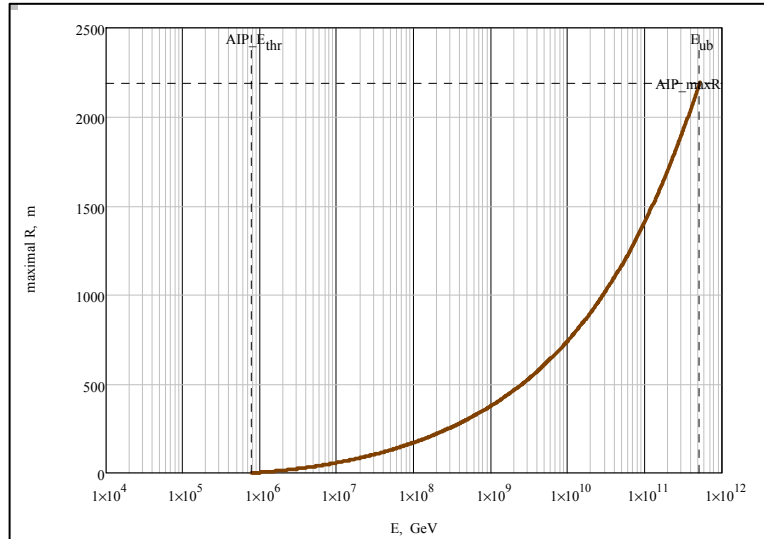


Figure 6. The energy dependence of the maximal distance from the AIP center to the EAS core intersection with the XY plane

The probability density function of the distances between the coordinate system origin and the EAS cores' points of intersection with the XY plane for the showers observable by the AIP goniometer

The probability density function ${}^{(AIP)}f_R(R)$ of the distances R to the cores of observable showers at AIP goniometer is shown in the **figure 7**.

This distribution is defined in the available distances interval

$$0 < R < {}^{(AIP)}\text{maxR}$$

$${}^{(AIP)}\text{maxR} = 2194 \text{ m}$$

The distance of most probable EAS observations is

$${}^{(AIP)}R_{\text{mode}} = 38.4 \text{ m}$$

The average distance is

$${}^{(AIP)}R_{\text{av}} = {}^{(AIP)}\langle R \rangle = 106.4 \text{ m}$$

The root mean square distance is

$${}^{(AIP)}R_{\text{rms}} = \sqrt{{}^{(AIP)}\langle R^2 \rangle} = 149.5 \text{ m}$$

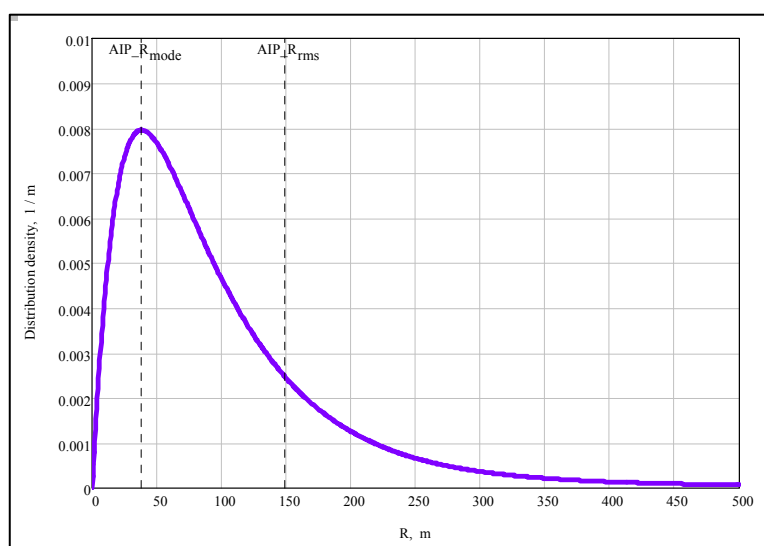


Figure 7. The distribution density of the EAS core distances R from the AIP goniometer center.

Two-dimensional distribution of the EAS core position points' observable by AIP goniometer

The diametrical section of two-dimensional distribution ${}^{(AIP)}f^{(2)}(x, y)$ of the EAS core position points' observable by AIP goniometer is shown in the **figure 8**.

The average position of all EAS cores' intersections with XY plane is obviously in the goniometer's center ($x = 0, y = 0$) and the standard deviation in each of (x, y) dimensions is equal to

$${}^{(AIP)}\sigma R = \sqrt{{}^{(AIP)}\langle R^2 \rangle / 2} = 105.7 \text{ m}.$$

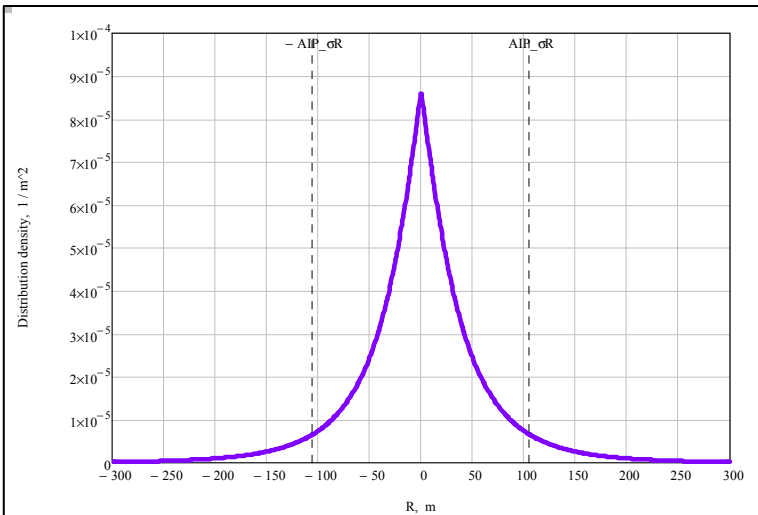


Figure 8. The diametrical section of the EAS core position points' distribution for the AIP goniometer observations.

Probability of the EAS core observation by the AIP goniometer at the distance less than R

The last probability is shown in the **figure 9**.

$${}^{(AIP)}F_R(R) = \int_0^R {}^{(AIP)}f_R(R') dR'$$

Approximately one-half fraction of the total number of EAS cores observable by the AIP goniometer are intersecting the XY plane within the distance of 77 m, while the 90% part intersects within the 215 m radius.

$${}^{(AIP)}F_R({}^{(AIP)}R_{\text{mode}}) = 21.9\%$$

$${}^{(AIP)}R_{\text{mode}} = 38.4 \text{ m}$$

$${}^{(AIP)}F_R({}^{(AIP)}\sigma R) = 64.7\%$$

$${}^{(AIP)}\sigma R = 105.7 \text{ m}$$

$${}^{(AIP)}F_R({}^{(AIP)}R_{\text{av}}) = 64.9\%$$

$${}^{(AIP)}R_{\text{av}} = 106.4 \text{ m}$$

$${}^{(AIP)}F_R({}^{(AIP)}R_{\text{rms}}) = 79.2\%$$

$${}^{(AIP)}R_{\text{rms}} = 149.5 \text{ m}$$

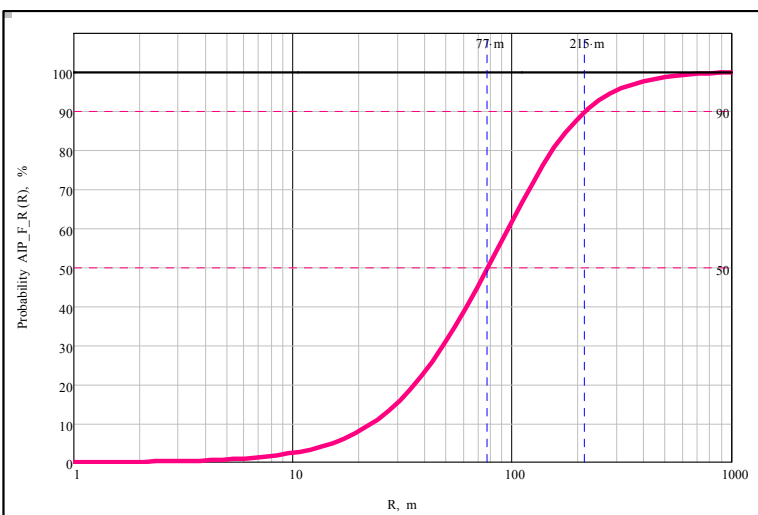


Figure 9. Probability of the EAS core observation by the AIP goniometer at the distance less than R

Borders of the areas of the observable vertical EAS cores' passage for the AIP goniometer

Those borders are shown in the **figures 10** and **11** for some maximal EAS energies.

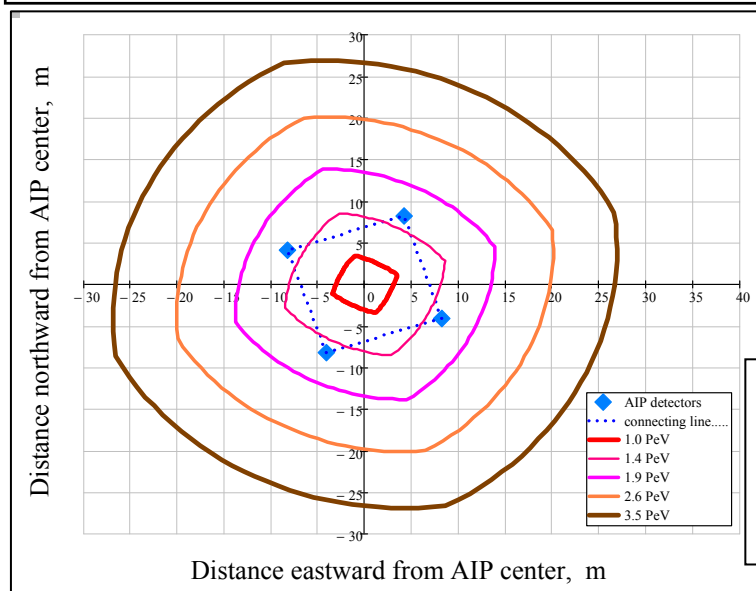
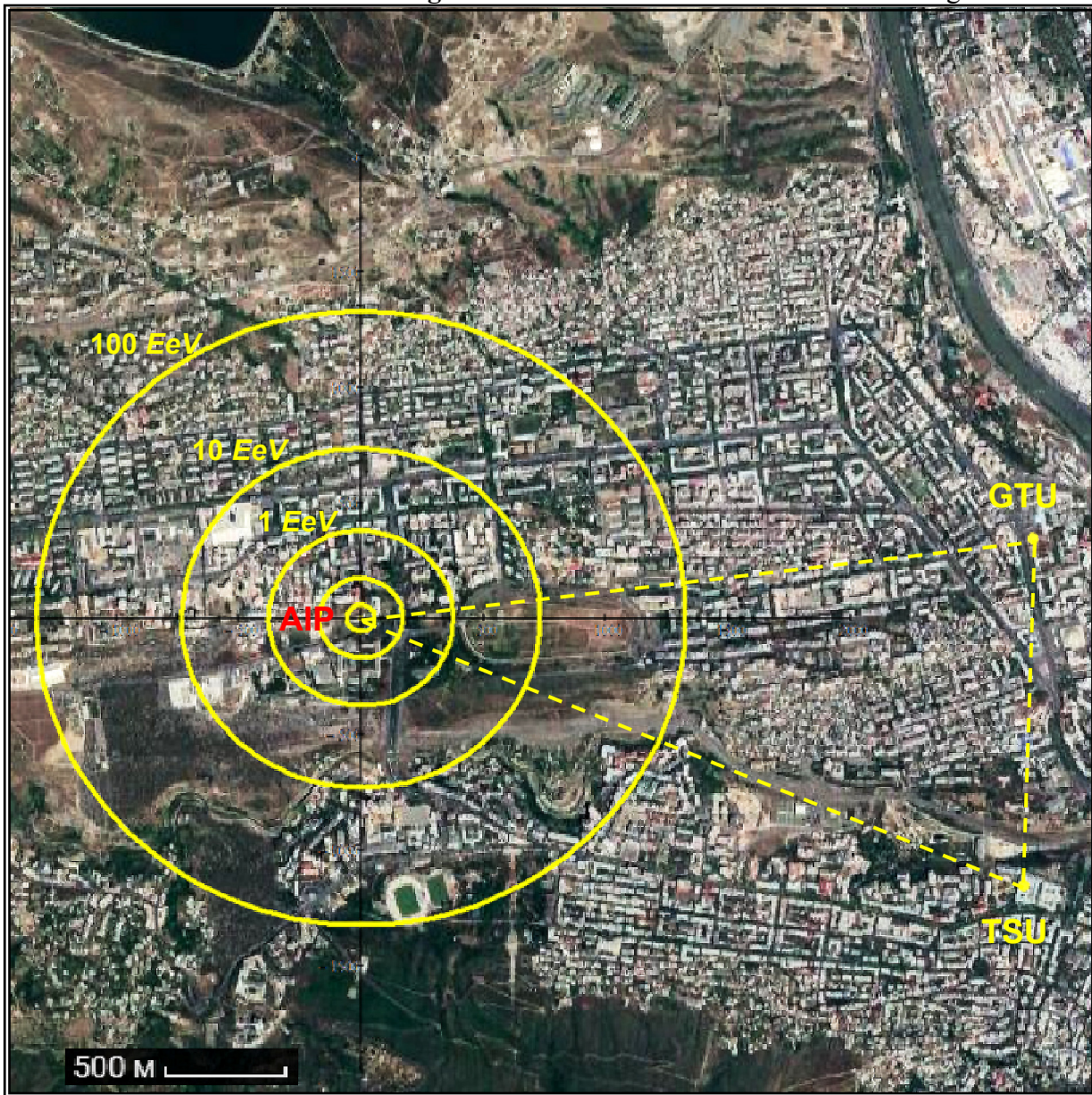


Figure 10 Borders of the areas of the AIP-observable vertical EAS cores' passage for the specified maximal total energies of the showers:
10PeV, 100PeV, 1EeV,
10EeV, 100EeV

Figure 11 Borders in the AIP vicinity of the areas of the observable vertical EAS cores' passage for the maximal total energies of the showers specified in the legend